

# A hidden constant in the anomalous Hall effect of a high-purity magnet MnSi.

Minhyea Lee<sup>1</sup>, Y. Onose<sup>1</sup>, Y. Tokura<sup>2,3</sup> and N. P. Ong<sup>1</sup>

<sup>1</sup>*Department of Physics, Princeton University, Princeton, NJ 08544, USA*

<sup>2</sup>*Department of Applied Physics, University of Tokyo, Tokyo 113-8656, Japan*

<sup>3</sup>*ERATO, JST, Spin Superstructure Project (SSS), Tsukuba 305-8562, Japan*

(Dated: February 6, 2008)

Measurements of the Hall conductivity in MnSi can provide incisive tests of theories of the anomalous Hall (AH) effect, because both the mean-free-path and magnetoresistance (MR) are unusually large for a ferromagnet. The large MR provides an accurate way to separate the AH conductivity  $\sigma_{xy}^A$  from the ordinary Hall conductivity  $\sigma_{xy}^N$ . Below the Curie temperature  $T_C$ ,  $\sigma_{xy}^A$  is linearly proportional to  $M$  (magnetization) with a proportionality constant  $S_H$  that is independent of both  $T$  and  $H$ . In particular,  $S_H$  remains a constant while  $\sigma_{xy}^N$  changes by a factor of 100 between 5 K and  $T_C$ . We discuss implications of the hidden constancy in  $S_H$ .

PACS numbers: 75.47.-m, 75.47.Np, 75.30.-m, 71.27.+a

The origin of the anomalous Hall (AH) effect in ferromagnets has been vigorously debated for the past 50 years. Karplus and Luttinger (KL) [1] proposed in 1954 that the AH current is an intrinsic current that is independent of the mean-free-path  $\ell$  [2, 3, 4, 5]. In the competing skew-scattering theory, the AH current arises from asymmetric scattering off impurities and defects, and is proportional to  $\ell$  [6]. While older experiments favor skew scattering, support for the KL/Berry-phase theory has been obtained from recent experiments [7, 8, 9, 10, 11, 12]. However, uncertainty remains on the relative importance of the 2 AH currents in pure systems (intrinsic regime), and on the role of extrinsic effects (impurities). Here, we show that the AH effect in a high-purity ferromagnet MnSi reveals a remarkable constancy. At temperatures  $T < T_C$ , the AH conductivity  $\sigma_{xy}^A$  is strictly proportional to  $M$  with a proportionality constant  $S_H$  that is independent of both  $T$  and magnetic field  $\mathbf{H}$ .

Conventionally, the observed Hall resistivity  $\rho_{yx}$  in a ferromagnet is written empirically as [13]

$$\rho_{yx} = R_0 B + \mu_0 R_s M \quad (1)$$

where  $R_0$  is the ordinary Hall coefficient,  $\mu_0$  the permeability and  $\mathbf{B} = \mu_0(\mathbf{H} + \mathbf{M})$  the induction field. The “anomalous Hall coefficient”  $R_s(T)$  is a scale factor that matches the  $M$ - $H$  curve to the anomalous part of the Hall resistivity  $\rho'_{yx} \equiv \rho_{yx} - R_0 B$ . As such,  $R_s(T)$  must be independent of the field  $B$ . AH measurements are routinely reported as a plot of  $R_s(T)$  vs.  $T$  as an empirical parameter. Yet, Eq. 1 has never been justified microscopically.

To distinguish between the two theories, we have focused on the intrinsic AH signal found in high-purity ferromagnets. In these systems, with large magnetoresistance (MR), the difficulties with Eq. 1 become acute. Additivity of currents in a solid implies that the total Hall conductivity is the sum  $\sigma_{xy} = \sigma_{xy}^N + \sigma_{xy}^A$  where  $\sigma_{xy}^N$  is the ordinary Hall conductivity. Additivity also requires that  $\sigma_{xy}^A$  be proportional to  $M$  [11, 12, 13, 14, 15], which

we express as

$$\sigma_{xy}^A = S_H M. \quad (2)$$

The scale factor  $S_H$  plays the central role in our analysis. Converting  $\sigma_{xy}$  to  $\rho_{yx}$ , we have

$$\rho_{yx} = R_0 B + S_H \rho^2 M \quad (3)$$

with  $\rho$  the resistivity and  $R_0 = \sigma_{xy}^N \rho^2 / B$  (we assume that  $\rho_{yx} \ll \rho$ ). We remark that Eq. 3 goes beyond just taking  $R_s$  to be  $\rho$  dependent (e.g. see Ref. [16]). When  $\rho$  varies strongly with  $H$ ,  $M$  fails to match  $\rho'_{yx}$  altogether, and  $R_s$  cannot be either defined or measured. This is especially so when  $\ell$  changes greatly with  $T$  and  $H$ . As we show, focusing on  $S_H$  uncovers the proper scaling between  $M$  and the AH response.

The metal MnSi, which displays one of the highest conductivities in a ferromagnet, has drawn intense interest because it exhibits non-Fermi liquid behavior at applied pressures above 14 kbar [17, 18]. Under hydrostatic pressure, it turns out that the Hall effect is indeed highly sensitive to the helical spin configuration, as discussed elsewhere [19]. At ambient pressure and zero  $H$ , MnSi undergoes a transition at  $T_C = 30$  K to a helical magnetic state with a long pitch  $\lambda$  ( $\sim 180$  Å) [20]. Neutron scattering experiments have established that, in a weak field ( $H < 0.1$  T), the spins cant towards the direction of  $\mathbf{H}$  to assume a conical structure and eventually align at  $H \sim 0.6$  T [21, 22].

The MnSi crystals were grown by the floating-zone method. Three crystals of area  $2 \times 1$  mm<sup>2</sup> and thickness 50-80  $\mu$ m were measured. At 4 K, values of  $\rho$  range from 0.4 to 5  $\mu\Omega$ cm. The residual resistivity ratio varies from 40 to 80. Contacts with contact resistance  $\leq 1 \Omega$  were made with Ag epoxy. Hall measurements were performed with the current (5 mA) applied parallel to the longest side ( $x$  axis), the field  $\mathbf{H}$  parallel to the shortest side ( $z$  axis) and Hall  $E$  field measured along  $\hat{y}$ . With field-sweep rates 0.05-0.1 T/min, we can resolve changes of  $\sim 2$  n $\Omega$  cm in  $\rho_{yx}$  at low  $T$ .  $M$  is measured in a SQUID magnetometer. Above 2 K, hysteretic behavior is not observed.

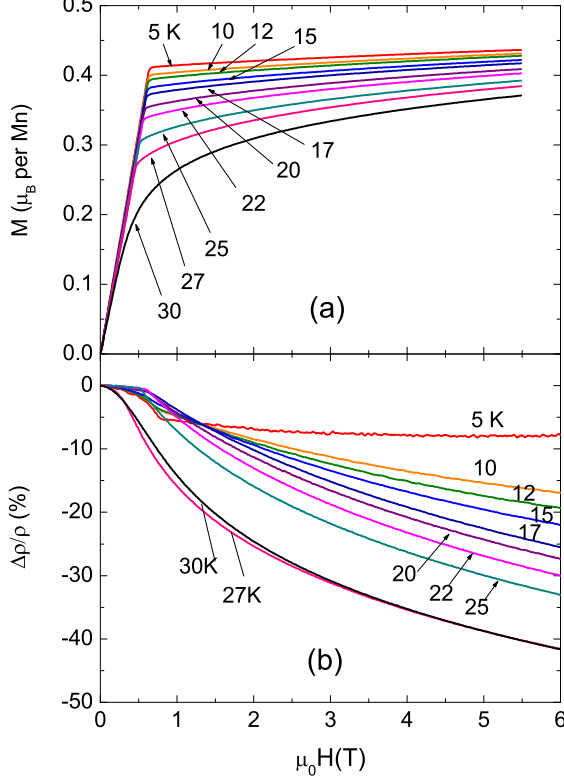


FIG. 1: (Color online) The magnetization curves  $M$  vs.  $H$  (Panel a) and curves of the relative magnetoresistance  $\Delta\rho/\rho$  (Panel b) in MnSi at selected  $T \leq T_C$  (30 K). Below  $T_C$  in Panel a, the linear increase in  $M$  up to the kink field  $H_k$  reflects the canting of the moments towards  $\mathbf{H}$ . In Panel b, the MR becomes large (40%) as  $T \rightarrow T_C$ . Above  $H_k$ ,  $M$  displays a negative curvature (especially near  $T_C$ ) whereas the curvature in  $\Delta\rho/\rho$  is positive.

As shown in the magnetization curves (Fig. 1a), the conical angle rapidly closes with field to produce the initial linear increase in  $M$ . The kink at  $H_k \sim 0.6$  T corresponds to alignment of the moments along  $\mathbf{H}$ .

Between  $T_C$  and 4 K,  $\rho$  in zero  $H$  decreases by a factor of 10. As shown below, this is entirely due to an increase in  $\ell$  (which reaches  $\sim 240$  Å at 4 K). Figure 1b shows that the MR is large ( $\sim 40\%$  near  $T_C$ , decreasing to 17% at 10 K at 6 T). The large changes in  $\rho$  with  $T$  and  $H$  make MnSi ideal for investigating how the intrinsic AH signal changes with carrier scattering time.

Curves of  $\rho_{yx}$  vs  $H$  are shown in Fig. 2 for  $T$  from 5 to 200 K. Above 150 K,  $\rho_{yx}$  is linear in  $H$ , consistent with hole-like carriers ( $\sigma_{xy} > 0$  and thus  $\rho_{yx} > 0$ ). As  $T$  decreases below 50 K, however,  $\rho_{yx}$  develops strong curvature in weak  $H$ . Below  $T_C$ ,  $\rho_{yx}$  acquires an AH term that – at first glance – seems to resemble  $M$  in accordance with Eq. 1. However, a more direct comparison reveals that the  $M$ – $H$  curves cannot be scaled to fit the

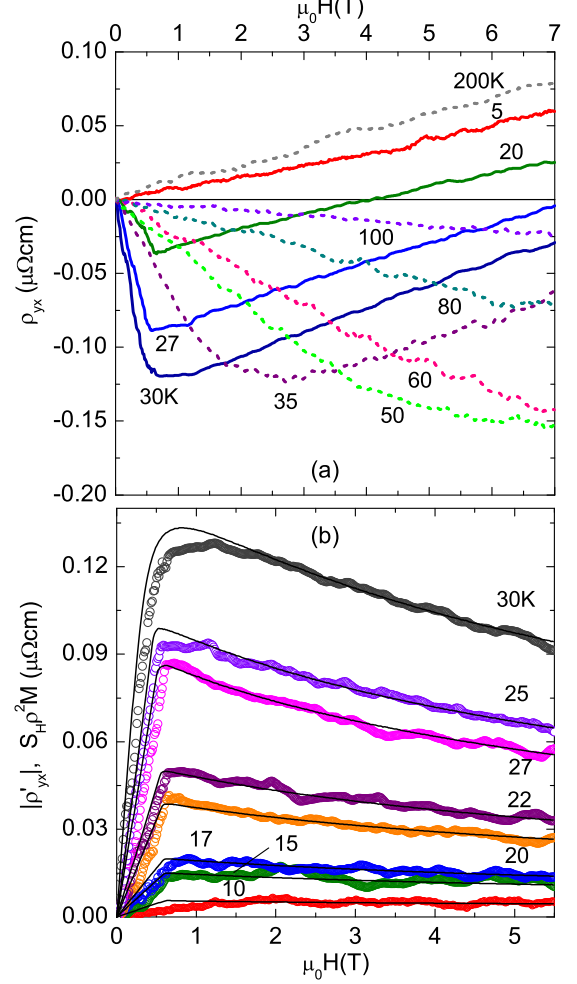


FIG. 2: (Color online) The observed Hall resistivity  $\rho_{yx}$  in MnSi at selected  $T$  (5–200 K, Panel a) and the fit of the anomalous part  $\rho'_{yx}$  to the modified magnetization profile  $\rho^2 M$  below  $T_C$  (Panel b). Panel a shows that  $\rho_{yx}$  is linear in  $H$  at high  $T$ , but gradually acquires an anomalous component  $\rho'_{yx} = \rho_{yx} - R_0 B$  with a prominent “knee” feature below  $T_C$ . In Panel b, at each  $T$ ,  $\rho'_{yx}$  (open circles) is fitted to the profile of  $\rho^2 M$  (solid curves), treating  $S_H$  and  $R_0$  as adjustable  $H$ -independent parameters. Note the positive curvature of the high-field segments.

curves of  $\rho'_{yx}$ . The reason is their opposite curvatures. The curvature of  $M$  is negative above  $H_k$ , whereas  $\rho'_{yx}$  displays positive curvature (Fig. 2b). The sign difference in the curvatures precludes definitively any satisfactory fit to Eq. 1.

Our approach is as follows. If Eq. 3 is correct, at each  $T < T_C$ , the profile of  $\rho'_{yx}$  vs.  $H$  must match that of  $\rho^2 M$  vs.  $H$  ( $S_H$  is taken to be  $H$ -independent). In this regard, it is reassuring that, unlike  $M$ , the product  $\rho^2 M$  shares the same curvature as  $\rho'_{yx}$ . By varying the

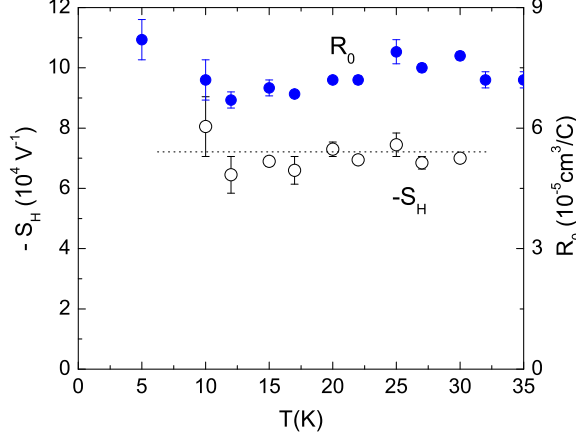


FIG. 3: (Color online) Values of the scale factor  $S_H$  (open circles) and the ordinary Hall coefficient  $R_0$  (solid circles) obtained from the fits shown in Fig. 2b. The average of  $S_H$  (dashed line) has the value  $-(7.06 \pm 0.48) \times 10^4 \text{ V}^{-1}$ . The average  $R_0$  gives a Hall density  $n_H = (8.53 \pm 0.07) \times 10^{22} \text{ cm}^{-3}$  and  $k_F \simeq 1.36 \times 10^8 \text{ cm}^{-1}$  in Sommerfeld approximation.

2 parameters  $R_0$  and  $S_H$ , we succeed in obtaining close fits at each  $T$ , as shown in Fig. 2b. The close match at each  $T$  provides strong evidence for the validity of Eq. 3. With  $R_0$  and  $S_H$  determined, the 2 Hall conductivities may be separated at each  $T$  (see below).

We have also searched for a skew-scattering contribution by adding an AH conductivity that scales as  $M$  and is linear in  $\ell$ . We write  $\sigma_{xy}^{sk} = \alpha S_H M \rho(0)/\rho(H)$ , where the dimensionless parameter  $\alpha(T)$  defines its magnitude at  $H = 0$  relative to the KL term, and  $\rho(0)/\rho(H)$  gives the  $H$  dependence of  $\ell$ . In Eq. 3, the second term is amended to  $S_H M \rho(H)^2 [1 + \alpha \rho(0)/\rho(H)]$ . We found that including  $\alpha$  did not improve the fits. Optimization leads to values of  $\alpha$  that fluctuate from 0 to 0.05 with no discernible trend (and consistent with  $\alpha = 0$ ).

As a consistency check, we note that the fits are physically meaningful only if both parameters turn out to vary only weakly with  $T$ , if at all. The variation of  $R_0$  and  $S_H$  obtained from the fits are plotted against  $T$  in Fig. 3. Within the scatter, the 2 parameters are virtually independent of  $T$ . The inferred  $R_0$  is nearly unchanged as  $T$  decreases from  $T_C$  to 5 K, despite the 10-fold decrease in  $\rho$ . This verifies our starting assumption that the decrease in  $\rho$  comes entirely from the increase in  $\ell$ , possibly reflecting suppression of scattering from spin fluctuations. From the Fermi wavevector  $k_F \sim 1.36 \times 10^8 \text{ cm}^{-1}$ , we find that the parameter  $k_F \ell$  varies from 330 to 30 between 4 K and  $T_C$ .

The constancy of  $S_H$  in Fig. 3 is more interesting and significant. As  $T$  decreases below  $T_C$ , both the magnetization and resistivity vary strongly with both  $H$  and  $T$ . Nonetheless, the AH conductivity is completely determined by  $M(T, H)$ , as expressed in Eq. 2. The con-

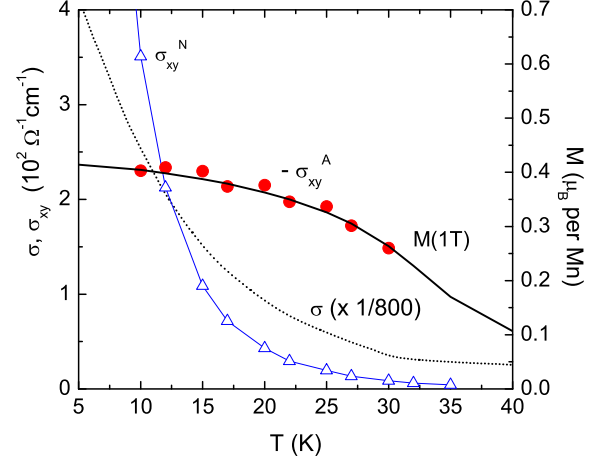


FIG. 4: (Color online) Comparison of the AH conductivity  $\sigma_{xy}^A$  (solid circles) with the ordinary Hall conductivity  $\sigma_{xy}^N$  (open triangles) in a 1-Tesla field (they have opposite signs).  $\sigma_{xy}^A$  is obtained from Eq. 2 using  $S_H$  shown in Fig. 3 and the measured  $M$  (solid curve), whereas  $\sigma_{xy}^N \sim \ell^2$  is calculated from  $R_0$ . As shown,  $\sigma_{xy}^A$  is strictly independent of  $\ell$ ; it changes slowly with  $T$  only because  $M(T)$  does. The  $T$  dependence of the conductivity  $\sigma \sim \ell$  (dashed curve) reflects  $\ell$  vs.  $T$ .

stancy of  $S_H$  implies that the dependence of  $\sigma_{xy}^A$  on  $T$  (or  $H$ ) derives entirely from that of  $M(T, H)$ . In particular, the 10-fold change in  $\ell$  below  $T_C$  has no observable effect on  $\sigma_{xy}^A$ . The task of predicting the AH conductivity in MnSi has been reduced to calculating one constant,  $S_H$ . This situation is in marked contrast to that presented by an analysis based on  $R_s(T)$  (Eq. 1).

It is instructive to compare directly the anomalous and ordinary Hall conductivities (Fig. 4). As the latter (calculated as  $\sigma_{xy}^N = R_0 B / \rho(H)^2$ ) increases as  $\sim \ell^2 H$ , it greatly exceeds the former in magnitude at low  $T$ . The two Hall conductivities are plotted in Fig. 4 with the field fixed at 1 T. As mentioned, below  $T_C$ ,  $\sigma_{xy}^A$  strictly follows the  $T$  dependence of  $M$  (solid curve), and is insensitive to the steep increase in  $\ell$  (the dashed curve shows the conductivity  $\sigma$ ). At 5 K,  $\sigma_{xy}^A$  attains the value  $240 (\Omega \text{ cm})^{-1}$ . By contrast,  $\sigma_{xy}^N$  is initially 20 times weaker than the AH term at  $T_C$ , but increases a 100-fold as  $T \rightarrow 5$  K and thus,  $\rho'_{yx}$  was not able to be detected in Fig. 2.

Our finding that  $\sigma_{xy}^A$  is nearly  $T$  independent disagrees with Ref. [14] which reports a strong deviation towards zero as  $T$  decreases to 5 K. Our conjecture for the discrepancy is that the quantity plotted in Fig. 5 of Ref. [14] is actually the absolute value of the total Hall conductivity  $|\sigma_{xy}| = |\frac{\rho_{yx}}{\rho^2}|$  (at a fixed field  $H = 0.1 \text{ T}$ ), rather than  $\sigma_{xy}^A$ . Between 30 and 5 K,  $\rho_{yx}$  measured at 0.1 T falls towards zero as  $T \rightarrow 5$  K (see Fig. 2 here), which implies that the total  $\sigma_{xy}$  does the same. It seems crucial to separate out the ordinary Hall current in MnSi. Another speculation for the discrepancy is that at the

low field of  $H = 0.1$  T as in Ref.[14], the contribution of the magnetization to AHE in MnSi may be non-trivial due to its helical nature. Thus, its contribution to  $\rho_{yx}$  can be different from that of fully ferromagnetic state in  $H > 0.6$  T, as we observed under hydrostatic pressure [19].

The relationship between the KL term and the Berry phase has been discussed by several groups [2, 3, 4, 5]. The curl of the Berry potential leads to an effective magnetic field  $\mathbf{\Omega}(\mathbf{k})$  in  $\mathbf{k}$  space that adds a new term to the group velocity, viz. (see Ref. [23] for an elementary treatment)

$$\hbar\mathbf{v}(\mathbf{k}) = \nabla_{\mathbf{k}}\epsilon(\mathbf{k}) + e\mathbf{\Omega}(\mathbf{k}) \times \mathbf{E}. \quad (4)$$

The anomalous term  $e\mathbf{\Omega} \times \mathbf{E}$ , which is transverse to  $\mathbf{E}$ , then gives a Hall conductivity that is independent of  $\ell$  (*i.e.* dissipationless).

The results in Fig. 4 showing that  $\sigma_{xy}^A$  is insensitive to the 10-fold change in  $\ell$  from 5 K to  $T_C$  provide compelling evidence in favor of the KL theory (and its Berry phase-based versions). However, present theories do not account for the broad interval of  $T$  over which  $\sigma_{xy}^A$  remains  $\ell$ -independent. How ubiquitous the constancy is (at low  $T$ ) in other ferromagnetic systems [15] and how it is modified at higher  $T$  are issues for further investigation (for e.g., in some ferromagnets,  $\rho'_{yx}$  changes sign near  $T_C$ ).

The experiment also addresses the relative importance of skew scattering compared to the KL term [24, 25, 26]. In recent calculations, the skew scattering term is either comparable to the KL term [25], or strongly dominant when  $k_{so}\ell > 1$  where  $k_{so} = E_{so}/v_F$ ,  $E_{so}$  and  $v_F$  are the

energy scale of spin-orbit interaction and Fermi velocity, respectively [26]. When the skew term is included, there is apparently no regime in which the KL term is clearly dominant (*i.e.*  $\sigma_{xy}^A$  strictly independent of  $\ell$ ).

By contrast, our results on MnSi show that, at all  $T < T_C$ ,  $\sigma_{xy}^{sk}$  is essentially unresolved and  $\sigma_{xy}^A$  is consistent with the KL term throughout the interval  $30 < k_F\ell < 330$ . In our experimental results,  $\sigma_{xy}^A$  still remains constant at  $T < T_C$ . This disagreement suggests either that skew scattering may have been greatly overestimated or that inelastic scattering may play a role at finite temperature[27].

Further understanding of the intrinsic AH conductivity requires measurements in high-purity crystals with large  $k_F\ell$  (in thin-film samples extrinsic scattering from the surface is problematic). We show that additivity of Hall currents provides the correct perspective to reconcile the large MR with the scaling between the AH current with  $M$ . The new analysis allows  $R_0$  (hence  $\sigma_{xy}^N$ ) to be isolated. More significantly, it uncovers a scaling factor  $S_H$  that is independent of both  $H$  and  $T$  below  $T_C$ . The skew scattering contribution is negligibly small (0–5 %). The constancy of  $S_H$  implies the AH current is completely determined by the curves of  $M$  vs.  $H$  below  $T_C$ . This simple scaling is obscured if  $\rho'_{yx}$  is forced to fit  $M$  in order to extract  $R_s$ , or if samples with large extrinsic scattering are used.

We have benefitted from useful discussions with N. Nagaosa and S. Onoda. Research at Princeton University was supported by the U.S. National Science Foundation (DMR 0213706).

- 
- [1] R. Karplus and J. M. Luttinger, Phys. Rev. **95**, 1154-1160 (1954).
  - [2] G. Sundaram and Q. Niu, Phys. Rev. B **59**, 14915-14925 (1999).
  - [3] M. Onoda and N. Nagaosa, J. Phys. Soc. Jpn. **71**, 19 (2002).
  - [4] T. Jungwirth, Q. Niu and A. H. MacDonald, Phys. Rev. Lett. **88**, 207208 (2002); Y. Yao, *et al.*, Phys. Rev. Lett. **92**, 037204 (2004).
  - [5] F. D. M. Haldane, Phys. Rev. Lett. **93**, 206602 (2004).
  - [6] J. Smit, Physica **21**, 877 (1955).
  - [7] P. Matl, N. P. Ong, Y. F. Yan, Y.Q. Li, D. Studtbeaker, T. Baum and G. Doubinia, Phys. Rev. B **57**, 10248-1025 (1998).
  - [8] Y. Taguchi, Y. Oohara, H. Yoshizawa, N. Nagaosa and Y. Tokura, Science **291**, 2573-2576 (2001).
  - [9] W.-L. Lee, S. Watauchi, V. L. Miller, R. J. Cava and N. P. Ong, Science **303**, 1647-1649 (2004).
  - [10] R. Mathieu, A. Asamitsu, H. Yamada, K. S. Takahashi, M. Kawasaki, Z. Fang, N. Nagaosa, Y. Tokura, Phys. Rev. Lett. **93**, 016602 (2004).
  - [11] C. Zeng, Y. Yao, Q. Niu, and H. H. Weitering, Phys. Rev. Lett. **96**, 037204 (2004).
  - [12] Y. Onose and Y. Tokura, Phys. Rev. B **73**, 174421 (2006).
  - [13] Hurd, C., *The Hall Effect in Metals and Alloys*, 153 – 182 Ch.5 (Plenum, New York 1972).
  - [14] N. Manyala, Y. Sidis, J. F. Ditusa, G. Aeppli, D. P. Young and Z. Fisk, Nature Materials **3** 255-262 (2004).
  - [15] A. Husmann and L. J. Singh, Phys. Rev. B **73** 172417 (2006).
  - [16] Y. Kats, I. Genish, L. Klein, J. W. Reiner and M. R. Beasley, Phys. Rev. B **70**, 180407 (2004); J. Kötzler and Woosik Gil, *ibid.* **72**, 060412(R) (2005)
  - [17] C. Pfleiderer, G. J. McMullan, S. R. Julian and G. G. Lonzarich, Phys. Rev. B **55**, 8330-8338 (1998).
  - [18] C. Pfleiderer, S. R. Julien and G. G. Lonzarich, Nature **414**, 427- 429 (2001).
  - [19] Minhyea Lee, W. Kang, Y. Onose and N. P. Ong, (to be published).
  - [20] Y. Ishikawa, Y. Noda, Y. J. Uemura, C. F. Majkzak and G. Shirane, Phys. Rev. B **31**, 5884-5893 (1985).
  - [21] Y. Ishikawa and M. Arai, J. Phys. Soc. Jpn. **53**, 2726-2733 (1984).
  - [22] C. Thessieu, C. Pfleiderer, A. N. Stepanov and J. Flouquet, J. Phys. : Condensed Matter **9**, 6677-6687 (1997).
  - [23] N. P Ong, and W.-L. Lee, cond-mat/0508236.
  - [24] P. Nozières, and C. Lewiner, J. Phys. (France) **34**, 901-915 (1973).

- [25] V. K. Dugaev, P. Bruno, M. Taillefumier, B. Canals, and C. Laroix, Phys. Rev. B **71**, 224423 (2005).
- [26] S. Onoda, , N. Sugimoto, and N. Nagaosa, Phys. Rev. Lett. **97**, 126602 (2006).
- [27] S. Onoda and N. Nagaosa, *private communication*.